Electronic Supplementary Material (ESI) for New Journal of Chemistry.
This journal is © The Royal Society of Chemistry and the Centre National de la Recherche Scientifique 2024

# Catalytic Ethynylation of Formaldehyde for Selective Propargyl Alcohol Production Using the Copper Metal Organic Framework HKUST-1

Wanxi Yang,[a] Wencai Peng,*[a,b] Han Li,[a] Jin Mao,[a] Liqiang Qian[a] and Qingyu Zhang[a]

[a] *School of Chemistry and Chemical Engineering, Shihezi University, Shihezi 832003, Xinjiang, China.*

[b] *Key Laboratory for Green Processing of Chemical Engineering of Xinjiang Bingtuan, Shihezi, Xinjiang, China.*

***Corresponding author: Wencai Peng**

Tel: +86 – 18409071980

E-mail: pengwencai@shzu.edu.cn (Wencai Peng)

**Table S1.** Experimental raw materials and sources 3
**Figure S1.** Preparation process of HKUST-1. 4
**Figure S2.** Gas chromatographic analysis of the reaction solution after the reaction of 4 wt% concentration of formaldehyde with acetylene followed by the addition of the internal standard 1,4-butanediol (BDO). 6
**Table S2.** Textural properties of Cu-MOFs synthesized with different ligands under the same copper source and with different copper sources under the same ligand. 6
**Table S3.** Catalytic performance of Cu-MOFs synthesized with different ligands under the same copper source and with different copper sources under the same ligand. 7
**Table S4.** Regression coefficients (A, B, C, D and E) of formation Enthalpy for acetylene, formaldehyde and propargyl alcohol.[2] 8
**Table S5.** Regression coefficients (A, B, C, D and E) of formation Gibbs free energy for acetylene, formaldehyde and propargyl alcohol.[2] 8
**Figure S3.** Graphs of $C_{HCHO,0} - C_{HCHO}$ versus t (red line) and $P_{C_2H_2,0} - P_{C_2H_2}$ versus t (bule line). 8
**Figure S4.** Graphs of $1/C_{HCHO} - 1/C_{HCHO,0}$ versus t (red line) and $1/P_{C_2H_2} - 1/P_{C_2H_2,0}$ versus t (bule line). 9
**Table S6.** Linear fitting results at different reaction temperatures. 10
**Table S7.** Calculation of the difference between the actual concentration of formaldehyde and the theoretical value per unit reaction time ($h^{-1}$) for the same initial acetylene pressure. 10
**Table S8.** Calculation of the difference between the actual acetylene pressure and the theoretical value per unit reaction time ($h^{-1}$) for the same initial formaldehyde concentration. 10

# 1. Materials and methods

## 1.1 Materials and instrumentation

All regents and raw materials were used as received without any further purification. Detailed information on the materials was shown in Table S1.

**Table S1.** Experimental raw materials and sources

| Chemical name | Source | Initial mass fraction purity |
|---|---|---|
| 1,3,5-benzenetricarboxylic acid | Adamas-beta | 99% |
| $Cu(NO_3)_2 \cdot 3H_2O$ | Adamas-beta | 99% |
| N,N-dimethylformamide | Tianjin Fuyu Fine Chemical Co. Ltd. | 99.5% |
| formaldehyde | General-reagent | 37.0-40.0% |
| acetylene | Shihezi Hongsheng Gas Station | 99.99% |

X-ray powder diffraction (XRD) patterns were recorded on a Bruker D8 Advance powder diffractometer using a Cu Kα radiation source. The diffractograms of the samples were obtained by scanning in the range of 5-90 $^{o}$ at a scanning speed of 2 $^{o}$/min.

Scanning electron microscopy (SEM) studies on a ZEISS Sigma 300 were carried out to obtain the surface morphology of the particles. Before test, the samples were coated with a thin layer of gold to enhance their electrical conductivity.

Nitrogen physisorption measurements were conducted using a Micromeritics ASAP 2460 apparatus. Before the adsorption analysis, the samples were degassed at 423.15 K for 6 h. Specific surface area was obtained from the 5-point Brunauer–Emmett–Teller (BET) procedure. The average pore diameter and pore volume were determined by the Barrett-Joyner-Halenda (BJH) method.

X-ray photoelectron spectroscopy (XPS) measurements were performed on a Thermo Scientific K-Alpha with an internally calibrated carbon deposit C 1s binding energy (BE) of 284.8 eV.

Fourier Transform Infrared (FT-IR) spectra obtained on a Thermo Scientific Nicolet 6700 instrument give the functional groups of the samples. The samples were dispersed on potassium bromide pallets and their infrared values in the range of 400-4000 $cm^{-1}$ were measured.

Comprehensive thermal analyzer HCT-1 from Beijing Hengjiu Experimental Equipment Co., Ltd was used for thermogravimetric analysis (TGA) under an air atmosphere with a heating rate of 10 K/min and a temperature range of 303.15-773.15 K.

A gas chromatograph (GC-2014C, Shimadzu, Japan) with a DB-WAX column of 15 m in length and 0.53 mm in diameter was used to analyze the content of propargyl alcohol (PA) and 1,4-butynediol (BYD).

## 1.2 Catalyst preparation

A crystalline porous metal-organic framework HKUST-1 by solvothermal method. The specific preparation process of the catalyst is shown in Figure S1. At room temperature, solution of $Cu(NO_3)_2 \cdot 3H_2O$ (4.832 g, 20 mmol) and 1,3,5-benzenetricarboxylic acid (2.101 g, 10 mmol) in N,N-dimethylformamide (DMF, 100 mL) was stirred for 0.5 h. After the solid was dissolved, it was placed into a constant temperature oven at 348.15 K and reacted for 24 h. After the solid was cooled down to room temperature, the blue product was filtered off and then washed with

deionized water, dried at 348.15 K overnight, followed by calcination in a muffle furnace at 473.15 K for 24 h. The sample obtained was labeled as HKUST-1.

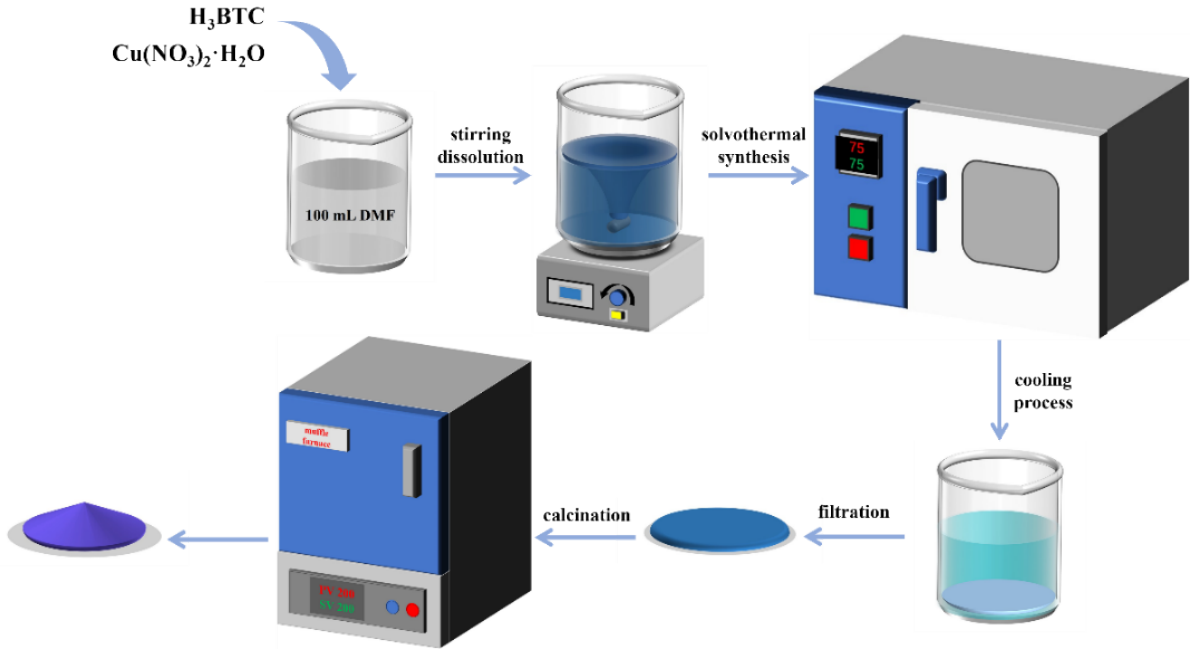


**Figure S1.** Preparation process of HKUST-1.

### 1.3 Catalytic activity evaluation

Ethynylation of formaldehyde was carried out in a 100 mL autoclave. 0.5 g of HKUST-1 and 35 mL of formaldehyde solution (0.4 wt%) were added to the autoclave at one time. Before the reaction, $N_2$ was introduced to the autoclave to purge the air and then replaced with $C_2H_2$. After setting a prescribed $C_2H_2$ pressure, the temperature was raised to 348.15 K with stirring at 600 r/min for 0.5 h to activate the catalyst. The mixture was then stirred continuously and heated to the prescribed temperature while the reaction time was started. At the end of the reaction, the reactor was turned off and the solution was cooled down to room temperature. After filtering the mixture, the filtrate was analyzed in two ways. One involved determining the formaldehyde content of the reaction solution before and after the reaction by titration with sodium sulfite and deriving the formaldehyde conversion from Equation (S1). The other way was used to analyze the content of propargyl alcohol (PA) and 1,4-butynediol (BYD) on a gas chromatograph (GC-2014C), as shown in Equations (S2) and (S3), respectively. Furthermore, the selectivity of PA and BYD can be calculated based on Equations (S2) and (S3) as shown in Equation (S4) and (S5), respectively.

$$X = \frac{m_0\omega_0 - m_1\omega_1}{m_0 w_0} \times 100\% \tag{S1}$$

$$Y_{PA} = \frac{M_{HCHO} \times m_{PA}}{M_{PA} \times m_0 w_0} \times 100\% \tag{S2}$$

$$Y_{BYD} = \frac{2 \times M_{HCHO} \times m_{BYD}}{M_{BYD} \times m_0 w_0} \times 100\% \tag{S3}$$

$$S_{PA} = \frac{Y_{PA}}{Y_{PA} + Y_{BYD}} \times 100\% \quad \textbf{(S4)}$$

$$S_{BYD} = \frac{Y_{BYD}}{Y_{PA} + Y_{BYD}} \times 100\% \quad \textbf{(S5)}$$

Here, X = conversion rate of formaldehyde, %.
$m_0$ = mass of reaction solution before reaction, g.
$\omega_0$ = mass fraction of formaldehyde in the initial reaction solution, %.
$m_1$ = mass of filtrate used for titration, g.
$\omega_1$ = mass fraction of formaldehyde in the filtrate, %.
$Y_{PA}$ = yield of PA, %.
$M_{HCHO}$ =molar mass of formaldehyde, mol/g.
$m_{PA}$ = mass of PA in the reaction solution, g.
$M_{PA}$ = molar mass of PA, g/mol.
$Y_{BYD}$ = yield of BYD, %.
$m_{BYD}$ = mass of BYD in the reaction solution, g.
$M_{BYD}$ = molar mass of BYD, g/mol.
$S_{PA}$ = selectivity of PA, %.
$S_{BYD}$ = selectivity of BYD, %.

### 1.4 Computational methods

Calculations of Gibbs free energies of reactants and products on HKUST-1 were carried out in Gaussian 16 program package[1]. In the geometrical optimisations of reactant molecules or product molecules adsorbed on HKUCT-1 at B3LYP/6-311++G (2d, P) using density functional theory and no geometric constraints are imposed. The reasonableness of the configurations obtained (no false frequencies) was also confirmed by means of frequency calculations. The Gibbs free energy (EE + thermal free energy correction) in the extracted output was used to calculate the Gibbs free energy of adsorption ($\Delta G_{ads}$) as shown in Equation (S6), which unit is kJ/mol.

$$\Delta G_{ads} = G_{ads-state} - G_{reactant\ or\ product} - G_{Catalyst} \quad \textbf{(S6)}$$

$G_{ads-state}$ is the whole energy of the reactant or production and catalyst system, $G_{reactant\ or\ product}$ is the energy of the single reactant or production, and $G_{Catalyst}$ is the energy of HKUST-1.

### 1.5 Gas chromatography analysis

The gas chromatogram analysis of the reaction solution after the reaction of 4 wt% concentration of formaldehyde with acetylene followed by the addition of the internal standard 1,4-butanediol (BDO) is shown in Figure S2. The retention times of formaldehyde, methanol, propargyl alcohol (PA), 1,4-butanediol (BDO) and 1,4-butynediol (BYD) were 0.4 min, 0.7 min, 5.3 min, 11.6 min and 25.6 min, respectively.

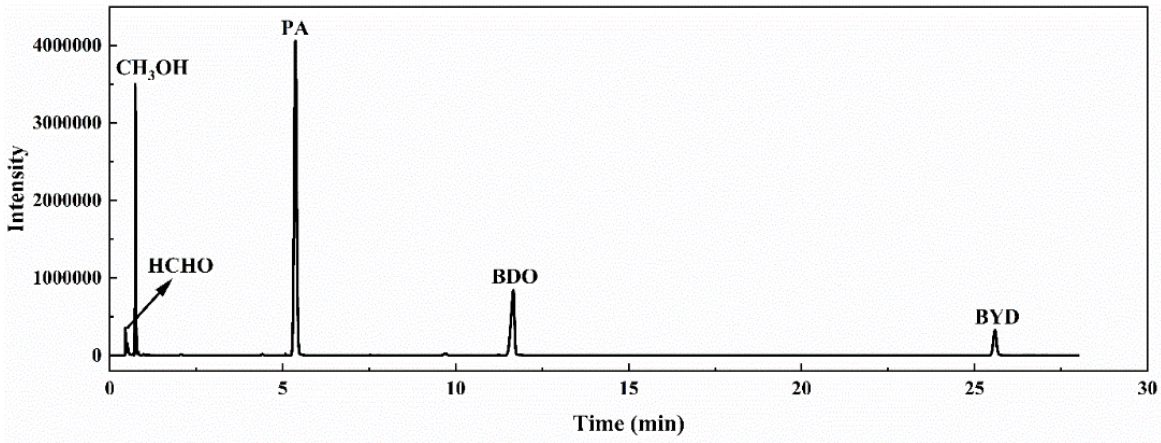


**Figure S2.** Gas chromatographic analysis of the reaction solution after the reaction of 4 wt% concentration of formaldehyde with acetylene followed by the addition of the internal standard 1,4-butanediol (BDO).

**Table S2.** Textural properties of Cu-MOFs synthesized with different ligands under the same copper source and with different copper sources under the same ligand.

| Entry | Copper source | Ligand | $S_{BET}$ ($m^2/g$) | $D_{pore}$ (nm) | Average Size (nm) |
|---|---|---|---|---|---|
| 1 | $Cu(NO_3)_2 \cdot 3H_2O$ | 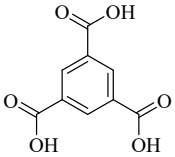 | 1488.03 | 0.774 | 3.8 |
| 2 | $Cu(NO_3)_2 \cdot 3H_2O$ | 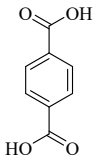 | 20.33 | 0.054 | 25.8 |
| 3 | $Cu(NO_3)_2 \cdot 3H_2O$ | 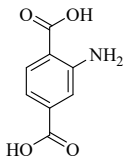 | 15.28 | 0.057 | 21.6 |
| 4 | $Cu(NO_3)_2 \cdot 3H_2O$ | 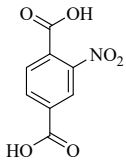 | 8.75 | 0.048 | 19.1 |
| 5 | $Cu(NO_3)_2 \cdot 3H_2O$ | 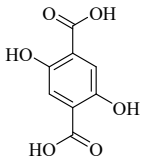 | 367.43 | 0.518 | 6.0 |
| 6 | $Cu(C_2H_3O_2)_2$ | 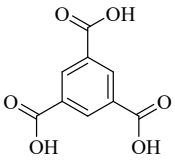 | 35.27 | 0.104 | 25.4 |
| 7 | $CuSO_4 \cdot 5H_2O$ | 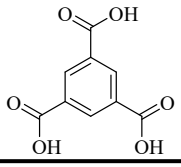 | 242.22 | 0.162 | 34.9 |

**Table S3.** Catalytic performance of Cu-MOFs synthesized with different ligands under the same copper source and with different copper sources under the same ligand.

| Entry | Copper source | Ligand | Formaldehyde conversion (%) | PA Yield (%) | BYD Yield (%) | Mole ratio of PA to BYD |
|---|---|---|---|---|---|---|
| 1 | $Cu(NO_3)_2 \cdot 3H_2O$ | 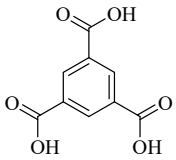 | 97.5 | 47.5 | 0.9 | 52.8 |
| 2 | $Cu(NO_3)_2 \cdot 3H_2O$ | 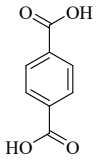 | 25.0 | 22.9 | 1.9 | 12.1 |
| 3 | $Cu(NO_3)_2 \cdot 3H_2O$ | 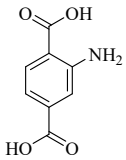 | 20.0 | 2.5 | 0.3 | 8.3 |
| 4 | $Cu(NO_3)_2 \cdot 3H_2O$ | 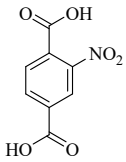 | 72.4 | 9.0 | 0.3 | 30.0 |
| 5 | $Cu(NO_3)_2 \cdot 3H_2O$ | 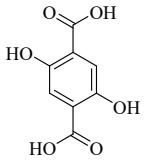 | 48.0 | 28.8 | 3.1 | 9.3 |
| 6 | $Cu(C_2H_3O_2)_2$ | 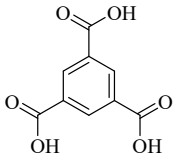 | 72.9 | 28.3 | 1.4 | 20.2 |
| 7 | $CuSO_4 \cdot 5H_2O$ | 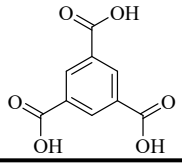 | 56.4 | 11.6 | 1.9 | 6.1 |

Reaction conditions: 0.5 g catalyst amount, 35 mL formaldehyde solution concentration (0.4 wt%), 0.2 MPa $C_2H_2$ initial pressure, 363.15 K reaction temperature, 6 h reaction time and 600 r/min stirring speed.

## 2. The Kinetic Study

The calculation of ΔH in Table 3 involved two main steps. First, the $H_f$ values of acetylene, formaldehyde and propargyl alcohol at different temperatures were found according to Table S4 and Equation (S7), and then the ΔH values of the reactions at different temperatures were found according to Equation (S8). The calculations of ΔG values in Table 3 were similar to those of ΔH, and the $G_f$ values of acetylene, formaldehyde and propargyl alcohol at different temperatures were first found according to Table S5 and Equation (S9), and then the ΔG values of the reactions at different temperatures were found according to Equation (S10). The data in Tables S4 and S5 can be consulted on the basis of the literature[2].

$$H_f = A + BT + CT^2 + DT^3 + ET^4 \quad \textbf{(S7)}$$

$$\Delta H(T) = H_{f,\ PA}(T) - H_{f,\ C_2H_2}(T) - H_{f,HCHO}(T) \quad \textbf{(S8)}$$

$$G_f = A + BT + CT^2 + DT^3 + ET^4 \quad \textbf{(S9)}$$

$$\Delta G(T) = G_{f,\ PA}(T) - G_{f,\ C_2H_2}(T) - G_{f,HCHO}(T) \quad \textbf{(S10)}$$

**Table S4.** Regression coefficients (A, B, C, D and E) of formation Enthalpy for acetylene, formaldehyde and propargyl alcohol.[2]

| Compound | $H_f = A + BT + CT^2 + DT^3 + ET^4$ ($H_f$: kJ/mol) | | | | |
|---|---|---|---|---|---|
| | A | B | C | D | E |
| Acetylene | 228.349 | 1.74E-03 | -8.69E-06 | 4.05E-09 | -5.05E-13 |
| Formaldehyde | -104.8 | -8.34E-03 | -2.11E-05 | 2.32E-08 | -6.66E-12 |
| Propargyl alcohol | 51.131 | -3.47E-02 | 1.64E-05 | -8.50E-10 | -8.15E-13 |

**Table S5.** Regression coefficients (A, B, C, D and E) of formation Gibbs free energy for acetylene, formaldehyde and propargyl alcohol.[2]

| Compound | $G_f = A + BT + CT^2 + DT^3 + ET^4$ ($G_f$: kJ/mol) | | | | |
|---|---|---|---|---|---|
| | A | B | C | D | E |
| Acetylene | 228.455 | -6.02E-02 | 1.57E-06 | 2.45E-09 | -9.75E-13 |
| Formaldehyde | -105.55 | -1.98E-03 | 4.86E-05 | -2.75E-08 | 6.10E-12 |
| Propargyl alcohol | 47.329 | 5.06E-02 | 8.13E-05 | -5.12E-08 | 1.23E-11 |

Here, $H_f$ = formation enthalpy of ideal gas for compound, kJ/mol.

A, B, C, D and E in Table S4 = regression coefficients of formation enthalpy for compound.

ΔH(T) = reaction enthalpy of formaldehyde ethynylation reaction to product propargyl alcohol at a temperature of T K, kJ/mol.

$G_f$ = formation Gibbs free energy of ideal gas for compound, kJ/mol;

A, B, C, D and E in Table S5 = regression coefficients of formation Gibbs free energy for compound.

ΔG(T) = Gibbs free energy of formaldehyde ethynylation reaction to product propargyl alcohol at a temperature of T K, kJ/mol.

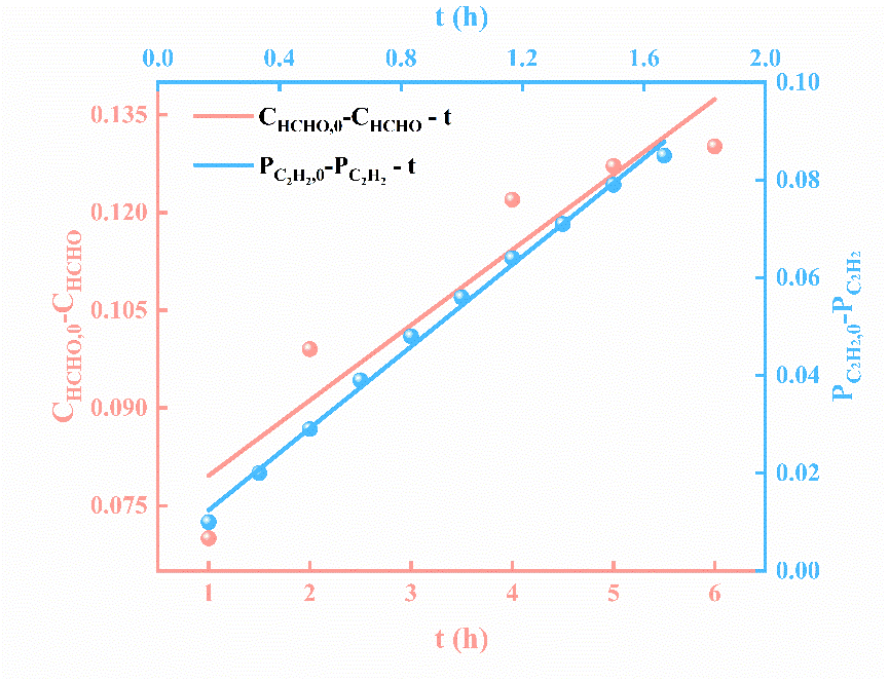


**Figure S3.** Graphs of $C_{HCHO,0} - C_{HCHO}$ versus $t$ (red line) and $P_{C_2H_2,0} - P_{C_2H_2}$ versus t (bule line).

Assuming a=0, the relationship between $C_{HCHO,0} - C_{HCHO}$ and t is

$$C_{HCHO,0} - C_{HCHO} = k_1 t + C \quad \textbf{(S11)}$$

where C is a constant. According to the formaldehyde concentration at different times, the relationship between $C_{HCHO,0} - C_{HCHO}$ and t is shown in Figure S3. The result of its linear fit is:

$$C_{HCHO,0} - C_{HCHO} = 0.068t - 0.012 \quad \textbf{(S12)}$$

and its linear correlation coefficient $R^2$ is 0.896.

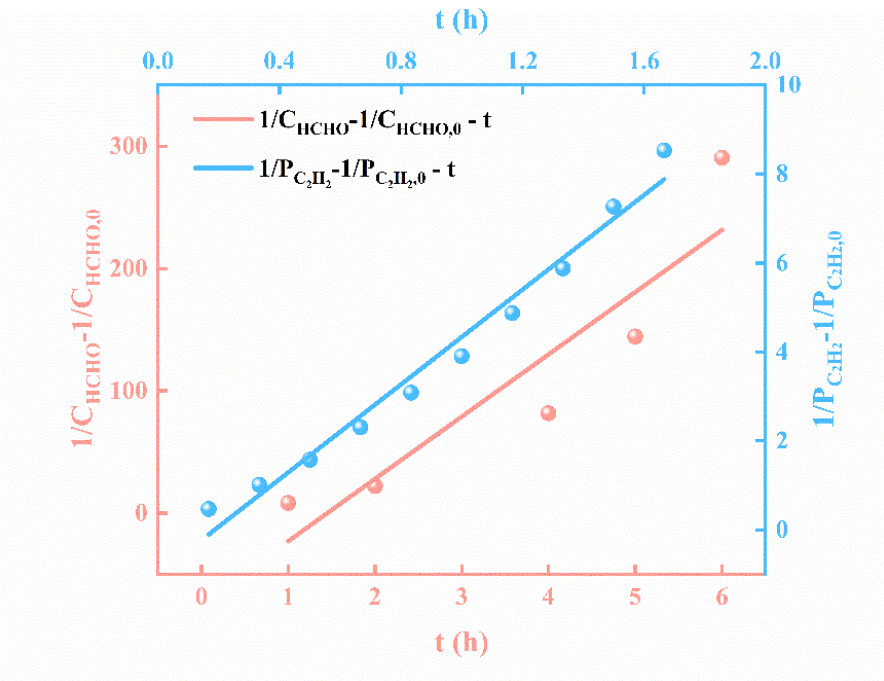

**Figure S4.** Graphs of $\frac{1}{C_{HCHO}} - \frac{1}{C_{HCHO,0}}$ versus $t$ (red line) and $\frac{1}{P_{C_2H_2}} - \frac{1}{P_{C_2H_2,0}}$ versus t (bule line).

Assuming a=2, the relationship between $\frac{1}{C_{HCHO}} - \frac{1}{C_{HCHO,0}}$ and t is

$$\frac{1}{C_{HCHO}} - \frac{1}{C_{HCHO,0}} = k_2 t + C \quad \textbf{(S13)}$$

where C is a constant. According to the formaldehyde concentration at different times, the relationship between $\frac{1}{C_{HCHO}} - \frac{1}{C_{HCHO,0}}$ and t is shown in Figure S4. The result of its linear fit is:

$$\frac{1}{C_{HCHO}} - \frac{1}{C_{HCHO,0}} = 50.878t - 73.687 \quad \textbf{(S14)}$$

and its linear correlation coefficient $R^2$ is 0.846.

Assuming b=0, the relationship between $P_{C_2H_2,0} - P_{C_2H_2}$ and t is

$$P_{C_2H_2,0} - P_{C_2H_2} = k_3 t + C \quad \textbf{(S15)}$$

where C is a constant. According to the pressure corresponding to different reaction times, the relationship between $P_{C_2H_2,0} - P_{C_2H_2}$ and t is shown in Figure S3. The result of its linear fit is

$$P_{C_2H_2,0} - P_{C_2H_2} = 0.05t + 0.004 \quad \textbf{(S16)}$$

and its linear correlation coefficient $R^2$ is 0.996.

Assuming b=2, the relationship between $\frac{1}{P_{C_2H_2}} - \frac{1}{P_{C_2H_2,0}}$ and t is

$$\frac{1}{P_{C_2H_2}} - \frac{1}{P_{C_2H_2,0}} = k_4 t + C \quad \textbf{(S17)}$$

where C is a constant. According to the pressure corresponding to different reaction times, the relationship between $\frac{1}{P_{C_2H_2}} - \frac{1}{P_{C_2H_2,0}}$ and t is shown in Figure S4. The result of its linear fit is

$$\frac{1}{P_{C_2H_2}} - \frac{1}{P_{C_2H_2,0}} = 5.322t - 0.989 \quad \textbf{(S18)}$$

and its linear correlation coefficient $R^2$ is 0.978.

**Table S6.** Linear fitting results at different reaction temperatures.

| T/K | $a$ | $k_{1/h^{-1}}$ | $R^2$ | $b$ | $k_{2/h^{-1}}$ | $R^2$ |
|---|---|---|---|---|---|---|
| 353.15 | 0 | 0.017 | 0.976 | 0 | 0.032 | 0.997 |
| 353.15 | 1 | 0.23 | 0.997 | 1 | 0.231 | 0.999 |
| 353.15 | 2 | 3.261 | 0.993 | 2 | 1.701 | 0.994 |
| 363.15 | 0 | 0.068 | 0.896 | 0 | 0.05 | 0.996 |
| 363.15 | 1 | 0.576 | 0.999 | 1 | 0.508 | 0.998 |
| 363.15 | 2 | 50.878 | 0.846 | 2 | 5.322 | 0.978 |

| | | | | | | |
|---|---|---|---|---|---|---|
| 373.15 | 0 | 0.036 | 0.862 | 0 | 0.069 | 0.994 |
| 373.15 | 1 | 0.955 | 0.993 | 1 | 0.948 | 0.999 |
| 373.15 | 2 | 46.21 | 0.811 | 2 | 13.395 | 0.984 |

**Table S7.** Calculation of the difference between the actual concentration of formaldehyde and the theoretical value per unit reaction time ($h^{-1}$) for the same initial acetylene pressure.

| Entry | $C_{HCHO,0}$ (mol/L) | Actual $C_{HCHO}$ (AC: mol/L) | Theoretical $C_{HCHO}$ $TC = \frac{C_{HCHO,0}}{e^{0.576t - 0.185}}$ (TC: mol/L) | Relative Error (RE) $RE = \frac{\lvert AC - TC \rvert}{TC}$ (RE: %) |
|---|---|---|---|---|
| 1 | 0.166 | 0.115 | 0.112 | 2.4 |
| 2 | 0.206 | 0.136 | 0.140 | 2.5 |
| 3 | 0.244 | 0.162 | 0.165 | 1.9 |
| 4 | 0.290 | 0.189 | 0.196 | 3.5 |
| 5 | 0.361 | 0.238 | 0.244 | 2.6 |

Reaction conditions: 0.5 g catalyst amount, 2 MPa $C_2H_2$ initial pressure, 363.15 K reaction temperature, 1 h reaction time and 600 r/min stirring speed.

**Table S8.** Calculation of the difference between the actual acetylene pressure and the theoretical value per unit reaction time ($h^{-1}$) for the same initial formaldehyde concentration.

| Entry | $P_{C_2H_2,0}$ (MPa) | Actual $P_{C_2H_2}$ (AP: MPa) | Theoretical $P_{C_2H_2}$ $TP = \frac{P_{C_2H_2,0}}{e^{0.508t - 0.033}}$ (TP: MPa) | Relative Error (RE) $RE = \frac{\lvert AP - TP \rvert}{TP}$ (RE: %) |
|---|---|---|---|---|
| 1 | 0.120 | 0.075 | 0.075 | 0.5 |
| 2 | 0.204 | 0.130 | 0.127 | 2.5 |
| 3 | 0.246 | 0.160 | 0.153 | 4.6 |
| 4 | 0.296 | 0.190 | 0.184 | 3.2 |
| 5 | 0.376 | 0.244 | 0.234 | 4.3 |

Reaction conditions: 0.5 g catalyst amount, 35 mL formaldehyde solution concentration (37 wt%), 363.15 K reaction temperature, 1 h reaction time and 600 r/min stirring speed.

## 3. References


1. M. J. Frisch, G. W. Trucks, H. B. Schlegel, et al., GAUSSIAN 16, Gaussian Inc., Walling ford CT, 2016.
2. C. L. Yaws, *The Yaws Handbook of Physical Properties for Hydrocarbons and Chemicals*, Gulf Publishing Company, Houston, 2005.